

<b>Zeitschrift:</b>	Schweizerische mineralogische und petrographische Mitteilungen = Bulletin suisse de minéralogie et pétrographie
<b>Band:</b>	78 (1998)
<b>Heft:</b>	3
<b>Artikel:</b>	Radiating cracks around chromite inclusions in olivine : constraints on P-T histories based on the thermoelastic properties of minerals
<b>Autor:</b>	Wendt, Anke S. / Altenberger, Uwe / D'Arco, Philippe
<b>DOI:</b>	<a href="https://doi.org/10.5169/seals-59294">https://doi.org/10.5169/seals-59294</a>

### **Nutzungsbedingungen**

Die ETH-Bibliothek ist die Anbieterin der digitalisierten Zeitschriften auf E-Periodica. Sie besitzt keine Urheberrechte an den Zeitschriften und ist nicht verantwortlich für deren Inhalte. Die Rechte liegen in der Regel bei den Herausgebern beziehungsweise den externen Rechteinhabern. Das Veröffentlichen von Bildern in Print- und Online-Publikationen sowie auf Social Media-Kanälen oder Webseiten ist nur mit vorheriger Genehmigung der Rechteinhaber erlaubt. [Mehr erfahren](#)

### **Conditions d'utilisation**

L'ETH Library est le fournisseur des revues numérisées. Elle ne détient aucun droit d'auteur sur les revues et n'est pas responsable de leur contenu. En règle générale, les droits sont détenus par les éditeurs ou les détenteurs de droits externes. La reproduction d'images dans des publications imprimées ou en ligne ainsi que sur des canaux de médias sociaux ou des sites web n'est autorisée qu'avec l'accord préalable des détenteurs des droits. [En savoir plus](#)

### **Terms of use**

The ETH Library is the provider of the digitised journals. It does not own any copyrights to the journals and is not responsible for their content. The rights usually lie with the publishers or the external rights holders. Publishing images in print and online publications, as well as on social media channels or websites, is only permitted with the prior consent of the rights holders. [Find out more](#)

**Download PDF:** 11.01.2026

**ETH-Bibliothek Zürich, E-Periodica, <https://www.e-periodica.ch>**

# Radiating cracks around chromite inclusions in olivine: constraints on P-T histories based on the thermoelastic properties of minerals

by Anke S. Wendt<sup>1</sup>, Uwe Altenberger<sup>2</sup> and Philippe D'Arco<sup>1</sup>

## Abstract

Radiating tensional cracks around chromite inclusions in forsterite-rich olivine porphyroclasts have been observed in the protomylonitic rim of a post-Variscan shear zone in the Finero peridotite complex (Ivrea Zone, northern Italy). These radial fractures developed during exhumation of the peridotite complex as a result of differences in the thermoelastic behavior of the chromite and the olivine.

The formation of radial cracks in the system chromite-olivine was calculated taking into account the contrast in thermal expansion, isothermal compressibility and shear modulus of both phases for retrograde P-T conditions encountered during exhumation. The pressure range of investigation was 0.7 GPa to 3.0 GPa at temperatures up to 1200 °C, representing average upper mantle P-T conditions. Olivine fracturing depended on the inclusion entrapment temperature and pressure; the slope of the retrograde P-T path was less important. Numerical calculations yielded a set of isocrack-lines with a negative  $\delta P/\delta T$  in a P-T grid. The position of the whole set of isocrack-lines on the P-T plane depended on the inclusion entrapment pressure and temperature. The calculated model can be used to estimate temperature and pressure appropriate to the following cases: (1) if independent evidence allows the determination of P-T conditions during crack formation, then the inclusion entrapment conditions can be calculated, (2) if the inclusion entrapment conditions and the retrograde path are known, the P-T conditions of crack formation can be determined.

For the Finero peridotite complex the dynamic recrystallization of olivine and the growth of antigorite + tremolite during a late metamorphism limited the lowermost P-T conditions for fracturing to 0.35 GPa and 550 °C. These values correspond to minimum inclusion entrapment conditions of  $P \approx 0.7$  GPa and  $T \geq 1000$  °C. The following exhumation history for the Finero peridotite complex is suggested: olivine and chromite crystallized at depths from 24 km to 30 km at temperatures from 1000 to 1200 °C. During exhumation, high temperature shearing started under granulite facies P-T conditions at around 19 km depth at temperatures from 775 to 940 °C. Further decrease of P and T produced the opening of radial cracks around chromite inclusions in olivine at more than 10 km depth and  $T \geq 550$  °C depending on the inclusion entrapment conditions.

**Keywords:** thermoelasticity, minerals, chromite inclusions, olivine, radial cracks, exhumation path, shear zone, Finero peridotite, Ivra zone.

## 1. Introduction

Radial cracks around inclusions in a matrix mineral were formerly considered to indicate the volume increase of mineral inclusions due to phase transformations such as the coesite-quartz transition (CHOPIN, 1984; GILLET et al., 1984; VAN DER MOLEN and VAN ROERMUND, 1986) and the  $\alpha$ - $\beta$

quartz transition (VAN DER MOLEN, 1981). Recent papers report also the occurrence of radial cracks during retrograde P-T evolutions around non-pseudomorphic single-phase inclusions of  $\alpha$ -quartz in garnet (WENDT et al., 1993) and chromite in olivine (WENDT and ALtenberger, 1994).

In this paper, we show how the relative volumetric variations of mineral inclusions (chromite)

<sup>1</sup> Ecole Normale Supérieure, Géologie, 24, rue Lhomond, F-75005 Paris, France.

Present address: University College London, Department of Geological Sciences, Rock and Ice Physics, Gower Street, London WC1E 6BT, U.K. <a.wendt@ucl.ac.uk>

<sup>2</sup> Institut für Geowissenschaften, Universität Potsdam, Postfach 601553, D-14415 Potsdam, Germany.

and their surrounding host phase (olivine) can be used to estimate P-T conditions during exhumation. The theoretical approach is based on a decrease in pressure and temperature which is externally controlled by the retrograde P-T path. During inclusion entrapment, pressure and temperature are the same in the host and in the inclusion, and correspond to peak pressure and temperature of the P-T path. During exhumation, the decrease of pressure and temperature will produce two retrograde P-T paths as a function of the volumetric variations of each mineral: (1) an external P-T path in the host and (2) an internal one in the inclusion. If the inclusion dilates more than the host mineral then an internal (over)pressure and a related linear increase in temperature in the inclusion will be created. If the overpressure is high, and can no longer be plastically accommodated by the host mineral, fractures will appear around the inclusion. At the moment of fracturing, again, the external and the internal pressure and temperature conditions in host and inclusion are equal.

Differences in volumetric variations for minerals depend on the thermoelastic properties of each mineral phase, i.e. the thermal expansion, the isothermal compressibility and the shear modulus. Therefore, cracks can be produced by a tensional stress developing at an inclusion-host interface during changing P-T conditions. Overpressure in an inclusion will result in radial cracks in the host mineral, underpressure in an inclusion will result in concentric cracks (inclusion shrinking).

Using the mathematical approach of VAN DER MOLEN and VAN ROERMUND (1986) and following the numerical model of WENDT et al. (1993), we studied the chromite-forsterite inclusion-host system. In this system, in contrast to previous studies (CHOPIN, 1984; GILLET et al., 1984; VAN DER MOLEN, 1981; VAN DER MOLEN and VAN ROERMUND, 1986; WENDT et al., 1993) the thermal dilation and compressibility of the host crystal are much higher than those of the inclusion.

The application of the model and the evolution of external and internal retrograde P-T paths in host minerals and their inclusions, are illustrated by chromite bearing olivine from a peridotite shear complex in the Ivrea Zone in northern Italy. Different retrograde P-T paths were modelled in order to evaluate the appearance of tensional cracks as a function of: (a) the initial temperature and pressure, and (b) the slope of the P-T path which describes the isothermal decompression component (a steep P-T path has a high isothermal decompression). The calculation is then discussed in light of petrological data and is finally

used to approximate the retrograde P-T path describing the exhumation of the peridotite complex.

## 2. Geological setting

The peridotite-bearing shear zone is situated in the Ivrea Zone within the internal part of the Western Alpine arc. The Ivrea Zone itself represents the exhumed area where the southern Alpine Moho as well as a part of the upper mantle came to the surface. Extensional exhumation (HANDY, 1987) started probably in the Early Permian (e.g. HENK et al., 1997) and ended in Alpine time (ZINGG et al., 1990; FRANZ et al., 1996). The Ivrea Zone contains ultramafic, mafic and sedimentary rocks metamorphosed under amphibolite to granulite facies conditions ( $T = 550^{\circ}\text{C}$  to  $940^{\circ}\text{C}$ , e.g. SCHMID and WOOD, 1976; SILLS, 1984; FRANZ et al., 1996;  $P = 400 \text{ MPa}$  to  $900 \text{ MPa} \pm 200 \text{ MPa}$ , FRANZ et al., 1996) mainly during post-Variscan time (e.g. KÖPPEL, 1974; ZINGG et al., 1990; HANDY and ZINGG, 1991). The metamorphic peak conditions increase from SE to NW. During pre-Alpine times, extensional crustal shearing in the lower to middle crust produced high-temperature ductile shear zones (BRODIE and RUTTER, 1987) which range from a few centimeters to several meters in width (e.g. ZINGG et al., 1990; ALTENBERGER, 1991).

The shear zone described here is situated within a phlogopite-rich peridotite of the Finero complex, and outcrops in the river bed of the Cannobina Valley 1 km southeast of Finero village (Fig. 1). Shearing occurred at high temperature under granulite facies conditions, and was followed by deformation under greenschist facies conditions. The peridotite samples examined in this study are taken from a 60 centimeter wide part of the shear zone system.

## 3. Petrography and microstructures of the chromite-olivine samples

The shear zone investigated is a low-angle normal ductile fault composed of a protomylonitic rim and an ultramylonitic centre. Extension during shearing occurred horizontally in a SW-NE direction. The shear zone dips steeply to the NNW, and the deformed peridotites show mineral stretching lineations and/or the elongation of porphyroclasts steeply plunging to the NW (ALTENBERGER, 1995) on their foliation planes. Extensive shearing in the peridotite complex started under granulite facies conditions at pressures of  $500 \text{ MPa}$  to  $750 \text{ MPa}$  and temperatures of  $>$

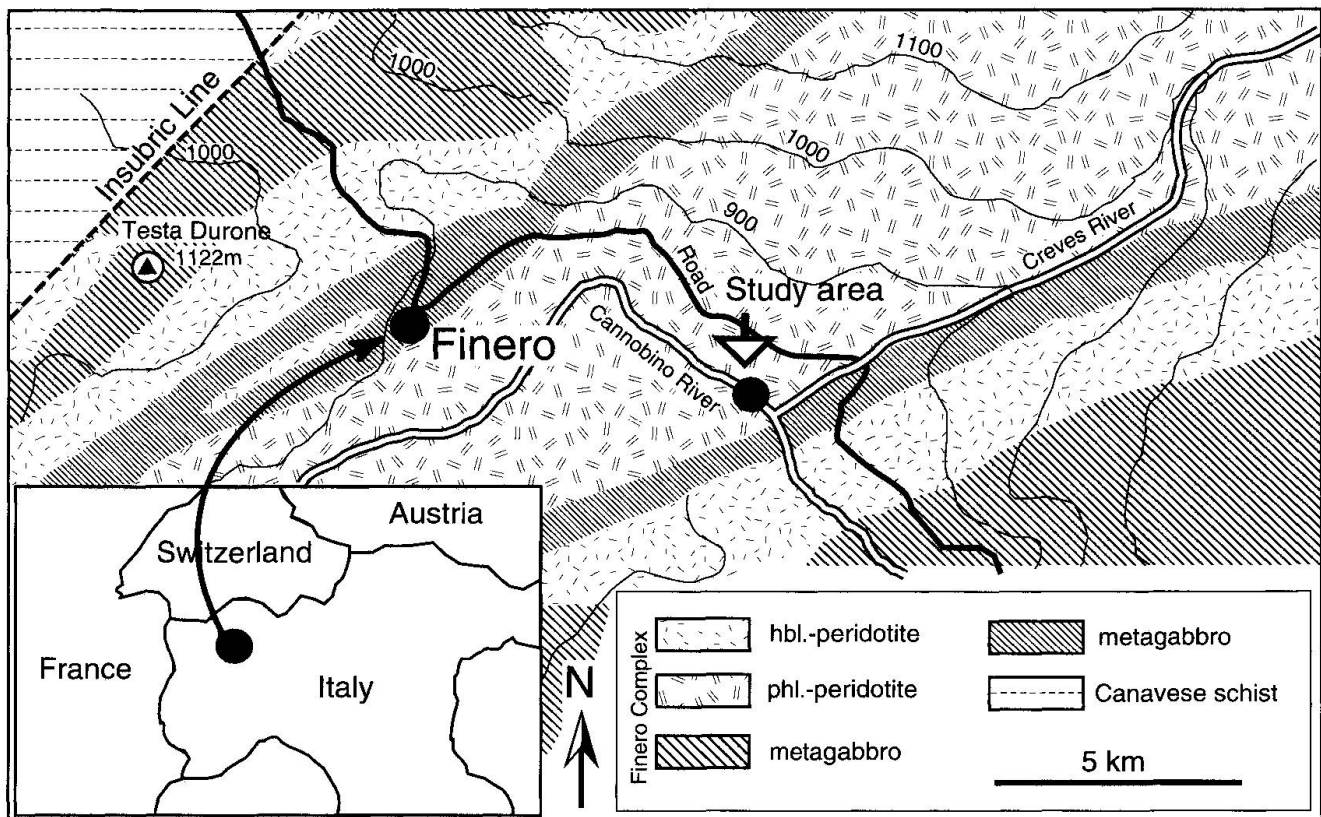


Fig. 1 Simplified geological map of the SW Finero Complex (modified from LENSCHE, 1968). The study area is located at the black circle.

775 °C (SCHMID and WOOD, 1976; SILLS, 1984; FRANZ et al., 1996), and continued under progressively decreasing P-T conditions. The high-temperature shearing is well preserved in the protomylonitic rim, whereas the lower temperature shearing is well preserved in the ultramylonitic center.

The main mineral phases in the center and rim of the peridotite complex are olivine ( $\text{Fo}_{91}$ ), orthopyroxene ( $\text{En}_{91} \text{Fs}_{8.5} \text{Wo}_{0.5}$ ) and phlogopite. Chromite and clinopyroxene ( $\text{Wo}_{49} \text{En}_{48} \text{Fs}_3$ ) are minor constituents. The chromites have a slightly different composition in the center ( $\text{Mg}_{0.48} \text{Fe}_{0.53}^{2+} \text{Fe}_{0.15}^{3+} \text{Cr}_{1.15} \text{Al}_{0.7} \text{O}_4$ ) and in the rim ( $\text{Mg}_{0.48} \text{Fe}_{0.53}^{2+} \text{Fe}_{0.13}^{3+} \text{Cr}_{1.1} \text{Al}_{0.8} \text{O}_4$ ) of the peridotite. The intensity of the deformation increases from the protomylonitic rim of the peridotite which is composed of relics of porphyroclasts to the ultramylonitic core whose composition is dominated by recrystallized grains and ductile deformation structures.

The olivine grains in the center and in the rim of the peridotite deformed by dislocation activities and by dynamic recrystallization. Dynamic recrystallization of olivine in the protomylonitic rim occurred only at the grain boundaries of the olivine porphyroclasts. Strong dislocation activities produced subgrain boundaries parallel to (100) probably by gliding on the systems (010)

(100) and  $\{0kl\}(100)$  (e.g. RALEIGH, 1968; CARTER and AVE LALLEMAND, 1970). Deformation lamellae or the appearance of cleavage planes in olivine were not observed. The chromite-crystals show no internal deformation, and are mostly round-shaped.

Small chromite inclusions (mean diameters: 0.15 mm, 0.21 mm, 0.12 mm, 0.25 mm) surrounded by approximately radially emanating cracks (Fig. 2) (WENDT and ALtenberger, 1994) were observed in large olivine porphyroclasts. Chromite inclusions in dynamically recrystallized olivine grains are not surrounded by fractures (Fig. 3). The radiating cracks in the porphyroclasts were filled with tremolite and antigorite fibers during a retrograde fluid-assisted metamorphism. Tremolite formed at the expense of pyroxene by the reaction:  $3 \text{ enstatite} + 2 \text{ diopside} + \text{SiO}_2 + \text{H}_2\text{O} \rightarrow \text{tremolite}$ .  $\text{SiO}_2$  was derived from phlogopite and probably from clinopyroxene, both depleted in  $\text{SiO}_2$  during metamorphic retrogression while the absolute  $\text{SiO}_2$  concentration of the sheared rock remained constant (ALtenberger, 1995). The formation of tremolite + forsterite at the expense of 5 enstatite + 2 diopside +  $\text{H}_2\text{O}$  was not observed. Antigorite was formed by the breakdown of olivine.

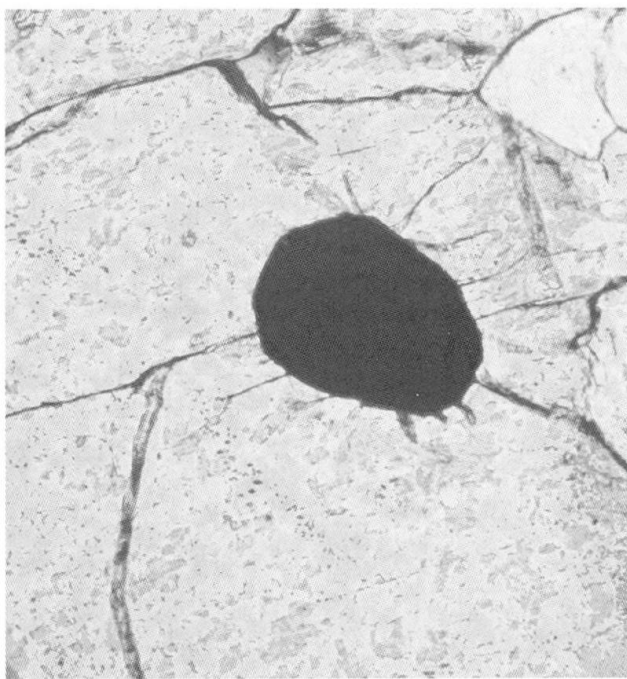


Fig. 2 Radiating tensional cracks around a chromite inclusion (dark) in an olivine porphyroblast (light) from the protomylonite. Microphotograph taken with crossed nicols (length: 0.58 mm).

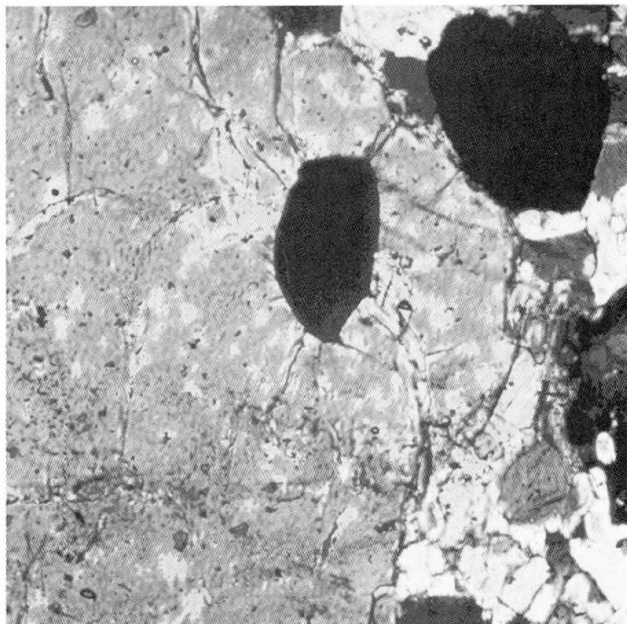


Fig. 3 Chromite crystal (dark) at the dynamically recrystallized rim of an olivine porphyroblast (light) from the protomylonite. Microphotograph taken with crossed nicols (length: 15.95 mm).

In contrast, the ultramylonitic center of the peridotite complex contains only recrystallized olivine; porphyroclasts are not preserved. Cracks around chromite inclusions in the recrystallized grains were not observed. This and the termina-

tion of the fractures whenever they meet recrystallized olivine grains (Fig. 3) suggest that the tensional cracks appeared before the dynamic recrystallization of olivine took place. The formation of tremolite through breakdown of pyroxene and the growth of antigorite by breakdown of olivine were also observed in the ultramylonitic center.

#### 4. Cracks around chromite inclusions in olivine – a model

The first elastic model for included minerals and their host minerals was developed by ROSENFELD (1969) who observed and calculated the appearance of radial stress-induced piezo-birefringent haloes around quartz inclusions in garnet. This model was later modified by VAN DER MOLEN (1981), GILLET et al. (1984), VAN DER MOLEN and VAN ROERMUND (1986) and WENDT et al. (1993). All their calculations are based on differential thermoelastic properties of the included mineral and its surrounding host mineral and are geometrically solved by considering the "sphere in hole" problem, as discussed by ROSENFELD (1969) (see also Appendix). We present here a thermoelastic model in the inclusion-host system chromite-olivine. The theoretical approach considers a spherical chromite located at the center of a spherical forsterite at initial pressure and temperature conditions  $P_i$  and  $T_i$ . Elastic behavior of inclusion and matrix is assumed for the P-T conditions encountered during exhumation. The chromite inclusion and the host olivine are considered to be perfectly elastic isotropic bodies. This assumption is justified even if local second-order effects arise from anisotropy, because they tend to cancel out over the bulk of the rock (VAN DER MOLEN, 1981). Pressure and temperature changes cause volume changes for each mineral in accordance with their thermoelastic properties (thermal expansion and isothermal compressibility, both opposite in sign, and the shear modulus). The theoretical approach shown here is similar to the one used for the geothermobarometer for quartz included in garnet (WENDT et al., 1993). In contrast to the quartz-in-garnet model, the host mineral here is more compressible than its inclusion: the chromite inclusion is half as compressible as the surrounding forsterite, and its thermal dilation is always smaller (see Appendix). Two limiting retrograde P-T paths for crack formation around chromite inclusions in olivine are considered: (1) At constant temperature and decreasing pressure, the inclusion expands less than the host creating concentric fractures grouped around the

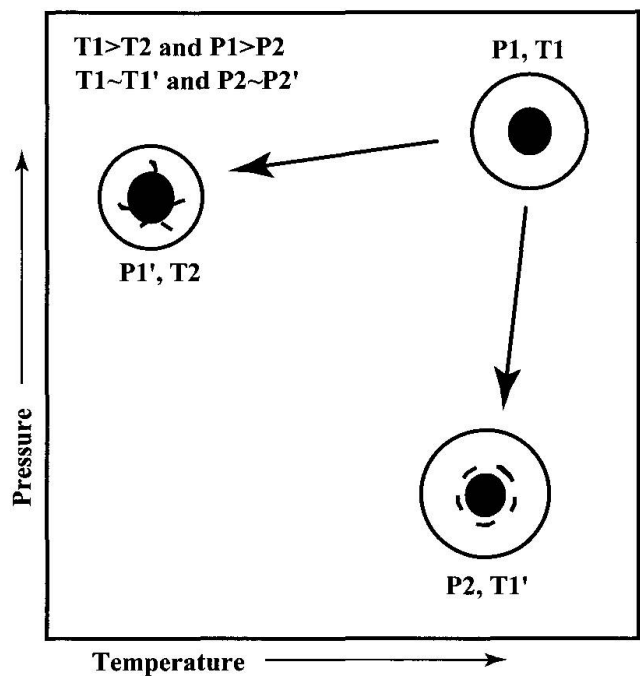


Fig. 4 The spherical model. Two limiting P-T paths. At initial conditions  $P_1, T_1$  the radius of a hypothetical hole in the olivine and the radius of the chromite inclusion are equal. At initial isobaric cooling the chromite tends to expand relatively against the olivine; radial cracks appear if the internal inclusion pressure increases to at least three times the pressure in the host. At initial isothermal decompression the olivine host expands more than the chromite inclusion creating concentric fractures.

inclusion (Fig. 4), (2) at constant pressure and decreasing temperature the inclusion compresses much less than the host. This leads to an overpressure in the inclusion with respect to the bulk host pressure. Radial stress effects appear when the tensional tangential stress at the inclusion-host interface becomes less than zero (Fig. 4). This occurs when the internal inclusion pressure rises to three times the externally applied pressure felt in the host mineral (e.g. VAN DER MOLEN, 1981) (details are given in the Appendix). Following the model of WENDT et al. (1993), we tested the relative volume evolution of host and inclusion and potential crack formation as a function of (1) the slope of the retrograde P-T paths, (2) the inclusion entrapment temperature, and (3) the inclusion entrapment pressure. The peak P-T conditions of the theoretical retrograde P-T paths are set to start at upper mantle conditions of 0.7 GPa to 3.0 GPa and 950 °C to 1200 °C, respectively.

In the first test, we set the entrapment conditions for all theoretical P-T paths at 2.0 GPa and 950 °C in order to study the appearance of radial cracks as a function of its retrograde slope

(= isothermal compressibility). The following theoretical P-T paths were considered (Fig. 5): (a) isobaric cooling followed by nearly isothermal decrease of pressure; (b, c) roughly linear decrease in pressure and temperature; and (d) isothermal decompression followed by linear decrease of pressure and temperature. The tests demonstrate that P-T paths with a higher component of isothermal decompression generate radial cracks at higher temperatures and lower pressures. The influence of the entrapment temperature conditions that create the required overpressure in the inclusion for radial crack generation was studied by considering again the retrograde paths described above (Fig. 5): They were then calculated for varying inclusion entrapment temperatures for the same entrapment pressure (2.0 GPa).

Both calculations showed that radial cracks form at pressures lower than 500 MPa and temperatures lower than 550 °C. For the same inclusion entrapment P-T conditions radial crack opening followed a line (A) with a negative  $\delta P/\delta T$  relationship. Those crack formation lines are reported here as isocrack-lines. The exact position of crack opening on the P-T plane is located at the intersection between the retrograde P-T path and the isocrack-line. Different inclusion entrapment temperatures for the same inclusion entrapment pressure produced a set of isocrack-lines (2.0 GPa, 950 °C = A, 2.0 GPa, 1000 °C = A', ...) with each line parallel to one another: at high entrapment temperature, fracturing occurred at higher P-T conditions than for low temperature entrapment conditions (Fig. 5).

The influence of the entrapment pressure was also studied on retrograde P-T paths equivalent to the paths described above. Entrapment pressures from 0.7 GPa to 3.0 GPa (Fig. 6) were numerically investigated. The calculation showed that the position of the set of isocrack-lines on the P-T plane varied as a function of the entrapment pressure: high inclusion entrapment pressure moved the set of isocrack-lines toward lower pressures and lower temperatures producing radial cracks at lower P-T conditions (Fig. 6). Low initial pressure moved the set of isocrack-lines toward higher pressures and higher temperatures producing radial cracks at higher P-T conditions (Fig. 6).

## 5. Discussion and application

The present study shows that the appearance of radiating tensional cracks depends on (i) the inclusion entrapment temperature and pressure conditions; (ii) the differential thermoelastic behavior of inclusion and host; and (iii) the isother-

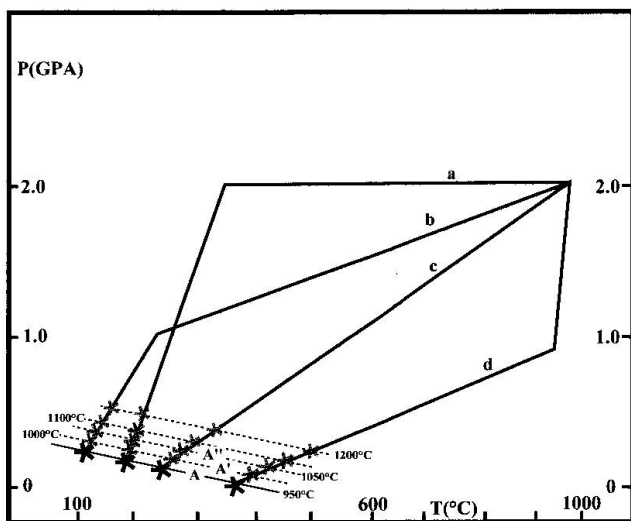


Fig. 5 The calculation of P-T paths with different slopes (decompression components) show that radial cracks appear at P-T conditions that are aligned on the P-T plane (line A). All retrograde P-T paths have the same starting conditions of 2.0 GPa and 950 °C. Radial fracturing (indicated by the stars) occurs whenever a retrograde P-T path of random shape intersects with the calculated line A. The initial temperature (950 °C, 1000 °C, 1200 °C) – related positions of the line A on the P-T plane is shown by the dashed lines (A', A''). The A, A', A'' lines together are named "isocrack-line set".

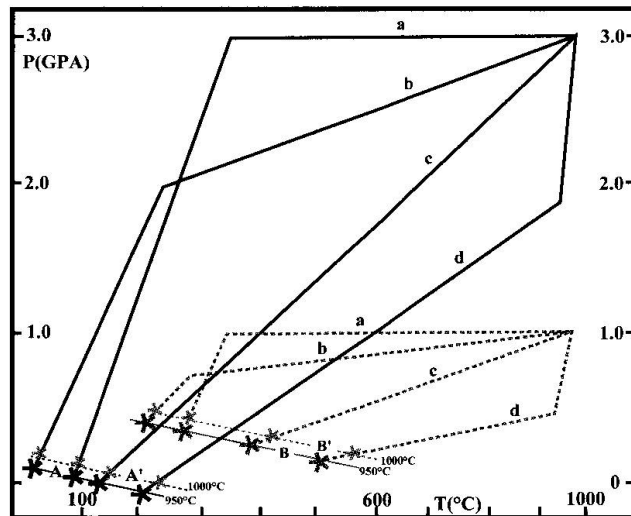


Fig. 6 Effects of initial entrapment pressure variations on radial crack opening. All P-T paths from figure 5 were studied using different inclusion entrapment pressures. The position of the set of isocrack-lines moves (i) toward lower pressures and temperatures for higher inclusion entrapment pressures (3.0 GPa) (set A) and (ii) toward higher pressures and temperatures for low inclusion entrapment pressures (1.0 GPa) (set B).

mal decompression expressed by the slope of the retrograde P-T path. The extrapolation of the so-obtained results to natural P-T paths is possible if (i) independent arguments allow the determina-

tion of the final P-T conditions during crack formation, then the entrapment conditions can be recalculated; (ii) the entrapment conditions and the retrograde path are known, then P-T conditions during crack formation can be determined. In the present case, the minimum P-T conditions for crack formation can be deduced from mineralogical evidence: firstly, radial cracks were never observed in dynamically recrystallized olivine from the protomylonite and the ultramylonite, and cracks terminate whenever they meet the dynamically recrystallized olivine grains. Secondly, the fractures are filled with antigorite and tremolite. The lower limit for dynamic recrystallization of olivine is reported to be between 550 °C and 950 °C (AVÉ LALLEMANT, 1970; KIRBY, 1983). In the Finero shear zone, the minimum P-T conditions for the dynamic recrystallization of olivine is constrained by the formation of antigorite which formed at the expense of the dynamically recrys-

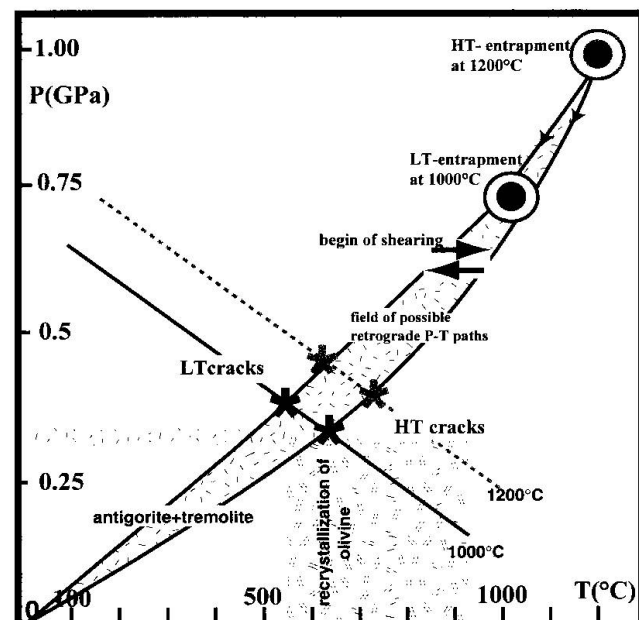


Fig. 7 Two possible retrograde P-T evolutions for the peridotite exhumation of the Finero area starting either at 24 km depth at T = 1000 °C or at 30 km depth at 1200 °C with the crystallization of olivine around chromite. 19 km, 775 to 940 °C: HT shearing,  $\geq 12$  km, 550 °C to 750 °C: appearance of radial cracks around chromite included in olivine (stars).  $< 12$  km,  $< 520$  °C: metamorphism in the stability field of antigorite + tremolite ( $X_{Mg\text{antigorite}} = 0.95$ ,  $X_{Mg\text{tremolite}} = 0.96$ ,  $X_{CO_2} \leq 0.05$ ). The dynamic recrystallization of olivine occurred during or after crack opening (see text for further explanations). (The upper stability limit of antigorite + tremolite was fixed after TROMMSDORFF and CONNOLLY, 1990; minimum dynamic recrystallization temperature of olivine after AVÉ LALLEMANT, 1970.) The two P-T paths describe limiting P-conditions for exhumation. Exhumation may have occurred on any similar P-T path situated in the field between them.

tallized olivine grains and tremolite. The latter grew syntectonically by the breakdown of clinopyroxene. The paragenesis of antigorite + tremolite has an upper stability limit of about 0.35 GPa and 520 °C ( $X_{\text{Mgantigorite}} = 0.95$ ,  $X_{\text{Mgtremolite}} = 0.96$ ,  $X_{\text{CO}_2} \leq 0.05$ ) (EVANS and TROMMSDORFF, 1977; TROMMSDORFF and CONNOLLY, 1990). Their crystallization in the radial cracks and throughout the peridotite matrix demonstrate that radial cracks opened before dynamic recrystallization of olivine occurred and before the growth of antigorite + tremolite; that is at P-T conditions equivalent or higher than 0.35 GPa and 550 °C. Such conditions lie in our model at the high temperature end of the isocrack-line B' in figure 6, and represent minimum inclusion entrapment P-T conditions from 0.7 GPa and  $T \geq 1000$  °C (Fig. 6). The result fits to the temperature dependent petrographic composition of the peridotite containing (olivine + orthopyroxene + phlogopite + clinopyroxene + chromite): Phlogopite-bearing dry peridotites form at temperatures around 1200 °C according to e.g. YODER and KUSHIRO (1969), MODRESKI and BOETTCHER (1972), and phlogopite-bearing wet peridotites form at temperatures around 1100 °C according to KUSHIRO (1970), MODRESKI and BOETTCHER (1972) and SATO et al. (1997). In addition, the position of crack opening on the P-T plane with P and T higher than 0.35 GPa and 550 °C, respectively, is characteristic for an exhumation path with a "medium" slope (Fig. 7). The so-described retrograde path includes the P-T conditions mentioned earlier for the shearing event at pressures and higher temperatures than 0.6 GPa and 775 °C, respectively. In conclusion, based on the new data set, the following P-T evolution for the peridotite complex is suggested (Fig. 7): crystallization of olivine around chromite started at depth between 24 km and 30 km corresponding to inclusion entrapment pressures of 0.7 GPa and 1.0 GPa, respectively, and temperatures from 1000 °C to 1200 °C. During exhumation, high temperature shearing took place at a depth of around 19 km at temperatures between 775 °C and 940 °C according to SCHMID and WOOD (1976), SILLS (1984), ALTENBERGER (1995) and FRANZ et al. (1996). A further decrease of pressure and temperature produced local tensional tangential stresses, so that radiating fractures opened around chromite inclusions in olivine: Cracking occurred at 10 km depth and  $T > 550$  °C for inclusion entrapment conditions of 1000 °C, 0.7 GPa, and at about 15 km depth and  $T < 750$  °C for inclusion entrapment conditions of 1200 °C and 1.0 GPa. The dynamic recrystallization of olivine and the fluid-enhanced growth of antigorite + tremolite occurred at minimum P-T

conditions of 0.35 GPa and 550 °C. The described linear to concave retrograde P-T evolution (Fig. 7) for shearing during exhumation of the peridotite complex is consistent with pressure-temperature-time rheological evolution during rifting of upper continental lithosphere as proposed by HANDY (1989). He explained the concave shape of the retrograde P-T evolution as being related to a fast rate of thermal equilibration compared to the rate of extensional shearing. The range of pressure and temperature conditions for the exhumation path of the Finero peridotite deduced from the differences of the thermoelastic properties of olivine and chromite suggest a similar relationship between the thermal equilibration and the shear deformation.

## 6. Concluding remarks

Chromite inclusions in forsterite-rich olivine from the Finero peridotite in the Ivrea Zone show that radial cracking in olivine depends predominantly on the thermal expansion and to a certain extent on the compressibility of both phases during retrograde P-T evolutions: the thermal dilatation of chromite is much smaller than that of olivine and its dilatation due to decompression is approximately half of that of the host. Consequently, when considering an extreme retrograde P-T path of isobaric cooling, the inclusion tends to contract less than the host resulting in an overpressure in the inclusion. This ultimately leads to the development of radial cracks emanating from the inclusion-host interface. In contrast, isothermal decompression should create concentric fractures around the inclusion, because the host-olivine expands more than the chromite inclusion. Generally, radial cracks in the inclusion-host system chromite-olivine describe entrapment pressures ranging from 0.7 GPa up to 3.0 GPa at inclusion entrapment temperatures up to around 1200 °C. Crack opening occurs at pressures between 0.05 GPa to < 0.6 GPa and temperatures from 40 °C to 750 °C on isocrack-lines with a negative  $\delta P/\delta T$  relationship. Petrological data are necessary to constrain one of the unknown parameters (P,T peak conditions or crack opening) which then allow the retrograde P-T evolution to be reconstructed.

## Acknowledgement

We wish to thank Bradley Hacker, Mark Handy, Gemma Keaney, Joern Kruhl, James Matthews, Martin Okrusch and Roland Oberhänsli for discussion, helpful comments and correcting the English.

## References

ALTENBERGER, U. (1991): Hochtemperierte Scherzonen in der Ivrea-Zone / N. Italien. *Zentralbl. Geol. Paläont.*, 3-20.

ALTENBERGER, U. (1995): Long-term deformation and fluid enhanced mass transport in a Variscan peridotite shear zone in the Ivrea Zone, northern Italy: a microtextural, petrological and geochemical study. *Geolog. Rd.*, 84, 3, 591-606.

AVÉ LALLEMAND, H.G. and CARTER, N.L. (1970): Syn-tectonic dynamic recrystallization of olivines and models of flow in the upper mantle. *Geol. Soc. Am. Bull.* 81, 2203-2220.

BRODIE, K.H. and RUTTER, E.H. (1987): Deep crustal faulting in the Ivrea zone of northern Italy. *Tectonophysics*, 140, 2-4, 193-212.

CHOPIN, C. (1984): Coesite and pure pyrope in high-grade blueschists of the Western Alps: a first record and some consequences. *Contrib. Mineral. Petrol.* 86, 107-118.

D'ARCO, Ph. and WENDT, A.S. (1994): Radial cracks around inclusions: a program to calculate P-T paths with respect to elastic properties of minerals. *Computer and Geosciences* 20, 9, 1275-1283.

DUFFY, TH.S. and ANDERSON, D.L. (1989): Seismic velocities in mantle minerals and the mineralogy of the upper mantle. *J. Geophys. Res.* 94, B2, 1895-1912.

EVANS, B.W. and TROMMSDORFF, V. (1970): Regional metamorphism of ultramafic rocks in the Central Alps: Parageneses in the system  $\text{CaO}-\text{MgO}-\text{SiO}_2-\text{H}_2\text{O}$ . *Schweiz. Mineral. Petrogr. Mitt.* 50, 481-492.

FRANZ, L., HENK, A., TEUFEL, S. and ONCKEN, O. (1996): Metamorphism of the Ivrea and Strona ceneri Zones (Northern Italy): Thermobarometry, geochronology and inferences about the crustal evolution. In: *Structures and properties of high strain shear zones in rocks*. Verbania. Abstr. Vol. 69.

GILLET, P., INGRIN, I. and CHOPIN, C. (1984): Coesite in subducted continental crust: P-T history deduced from a model. *Earth Planet. Sci. Lett.* 70, 426-436.

HANDY, M.R. and ZINGG, A. (1991): The tectonic and rheological evolution of an attenuated cross section of the continental crust: Ivrea crustal section, southern Alps, northwestern Italy and southern Switzerland. *Geol. Soc. Am. Bull.* 94, 236-253.

HANDY, M.R. (1989): Deformation regimes and the rheological evolution of fault zones in the lithosphere: the effect of pressure, temperature, grainsize and time. *Tectonophysics*, 163, 119-152.

HANDY, M.R. (1987): The structure, age and kinematics of the Pogallo fault zone, southern Alps, northwestern Italy. *Eclogae geol. Helv.* 80, 593-632.

HENK, A., FRANZ, L., TEUFEL, S. and ONCKEN, O. (1997): Magmatic underplating, extension and crustal reequilibration: Insights from a cross-section through the Ivrea zone and Strona-Ceneri zone, northern Italy. *J. Geol.* 105, 3, 367-377.

JAEGER, J.C. and COOK, N.G.W. (1979): *Fundamentals of Rock Mechanics*. 3rd ed., Chapman and Hall, New York.

KIRBY, S.H. (1983): Rheology of the lithosphere. *Rev. Geophys. Space Physics* 21, 1458-1487.

KÖPPEL, V. (1974): Isotopic U-Pb ages in monazites and zircons from the crust-mantle transition and adjacent units of the Ivrea and Ceneri zones, Southern Alps (Italy). *Contrib. Mineral. Petrol.* 43, 45-74.

KUSHIRO, I. (1970): Stability of amphibole and phlogopite in the upper mantle: Carnegie Inst. Washington Year Book 68, 245-247.

LENSCH, G. (1968): Die Ultramafite der Zone von Ivrea und ihre geologische Interpretation. *Schweiz. Mineral. Petrogr. Mitt.* 48, 91-102.

MODRESKI, P.J. and BOETTCHER, A.L. (1972): The stability of phlogopite and enstatite at high pressure: a model for micas in the interior of the earth. *Am. J. Science* 272, 852-869.

NUR, A. and SIMMONS, G. (1970): The origin of small cracks in igneous rocks. *Int. J. Rock Mech. Min. Sci.* 7, 307-314.

RALEIGH, C.B. (1968): Mechanisms of plastic deformation of olivine. *J. Geophys. Res.* 73, 5391-5406.

ROSENFELD, J. (1969): Stress effects around quartz inclusions in almandine and the piezothermometry of coexisting aluminium silicates. *Am. J. Sci.* 267, 317-351.

SCHMID, R. and WOOD, B. J. (1976): Phase relationships in granulitic metapelites from the Ivrea-Verbano Zone (Northern Italy). *Contrib. Mineral. Petrol.* 54, 255-279.

SILLS, J.D. (1984): Granulite facies metamorphism in the Ivrea zone, NW Italy. *Schweiz. Mineral. Petrogr. Mitt.* 64, 169-191.

SINGH, H.P. and SIMMONS, G. (1976): X-ray determination of thermal expansion of olivines. *Acta Cryst. A* 32, 771.

SKINNER, B.J. (1946): Thermal expansion. *Trans. British Ceram. Soc.* 45, 137. In: CLARK, S.J. (ed.): *Handbook of Physical Constants*. *Geol. Soc. Am. Mem.* 97.

TROMMSDORFF, V. and CONNOLLY, J. (1990): Constraints on phase diagram topology for the system  $\text{CaO}-\text{MgO}-\text{SiO}_2-\text{CO}_2-\text{H}_2\text{O}$ . *Contrib. Mineral. Petrol.* 104, 1-7.

VAN DER MOLEN, I. and VAN ROERMUND, H.L.M. (1986): The pressure path of solid inclusions in minerals: the retention of coesite inclusions during exhumation. *Lithos* 19, 317-324.

VAN DER MOLEN, I. (1981): The shift of the  $\alpha$ - $\beta$  transition temperature of quartz associated with thermal expansion of granite at high pressure. *Tectonophysics* 73, 323-342.

WENDT, A.S. and ALTENBERGER, U. (1994): Radial cracks around chromite inclusions in olivine from a Variscan peridotite shear zone in the Ivrea Zone, northern Italy. *Tectonophysics* 229, 133-137.

WENDT, A.S., D'ARCO, Ph., GOFFÉ, B. and OBERHÄNSLI, R. (1993): Radial cracks around  $\alpha$ -quartz inclusions in almandine: constraints on the metamorphic history of the Oman mountains. *Earth and Planet. Sci. Letters*, 114, 449-461.

YODER, M.S. Jr. and KUSHIRO, I. (1969): Melting of a hydrous phase: phlogopite. *Am. J. Sci.* 267, 558-582.

ZINGG, A., HANDY, M.R., HUNZIKER, J.C. and SCHMID, S. (1990): Tectonometamorphic history of the Ivrea Zone and its relationship to the crustal evolution of the Southern Alps. *Tectonophysics* 182, 169-192.

Manuscript received February 15, 1998; revision accepted September 10, 1998.

## Appendix

At initial conditions  $P_1$  and  $T_1$  a stress-free chromite grain is included in a growing forsterite-rich olivine. Both minerals are subjected to the same variations in externally controlled hydrostatic  $P$  and  $T$ . At initial conditions  $(P_1, T_1)$  the boundary of the chromite inclusion is considered to be superimposed on the boundary of an imagined hole in the olivine from whose constraining effect the chromite has been freed (sphere in hole problem, ROSENFELD, 1969).

To simplify the model and the following calculation the chromite inclusion is located at the center of the olivine and both phases are considered to be elastic isotropic bodies. It is assumed that elastic behavior is valid for the  $P$ - $T$  range encountered during the considered part of a retrograde pressure-temperature evolution.

With these assumptions, and at initial conditions  $(P_1, T_1)$ , the radii of the hole in the olivine and of the chromite are equal. At changing  $P$  and  $T$  the relative variation of the volume of each mineral depends on the thermal expansion, the isothermal compressibility and the shear modulus. The host olivine is much more compressible than the chromite inclusion and its thermal dilatation is always higher than that of the chromite. Therefore, two limiting cases can be considered. At constant temperature and decreasing pressure, the host will expand and the volume of the inclusion is always smaller than that of the olivine hole. This leads to an underpressure in the inclusion with respect to the whole rock pressure and concentric fractures around the inclusion may appear (Fig. 4). Along an isobaric cooling path the host (and the hole in the host) will shrink about two times more than the inclusion for the same  $P$ - $T$  variations. That leads to the required overpressure in the inclusion and radial cracks propagating from the host-inclusion-interface may develop.

The mathematical procedure used to solve the problem posed above was developed by VAN DER MOLEN (1981) and follows the notation of JAEGER and COOK (1972). It is based on the following idea: A spherical mineral with the radius  $R$  is included in a spherical matrix with the radius  $r$  ( $0 < r < \infty$ ,  $R \leq r$ ). In the calculation, stresses and pressures are positive for compression and negative for elongation and expansion. Two cases can be considered:

(1) Pressure exists only in the inclusion ( $P_{in}$ ), then the normal stress is

$$\sigma^r = P_{in} \cdot (R^3/r^3),$$

and the tangential stress

$$\sigma^t = -P_{in} \cdot (R^3/2r^3)$$

for conditions at the surface of the inclusion the normal stress becomes

$$\sigma^r = P_{in}$$

and the tangential stress

$$\sigma^t = -P_{in}/2$$

and

$$P_{infinite}^{host} = 0$$

2) Pressure exists in the matrix ( $P$ ) and the inclusion pressure is zero. Then the normal stress is

$$\sigma^r = P \cdot (1 - R^3/r^3),$$

and the tangential stress

$$\sigma^t = P (1 + R^3/2r^3)$$

For conditions at the surface of the inclusion, the

normal stress becomes

$$\sigma^r = 0$$

and the tangential stress

$$\sigma^t = 3P/2$$

Case (1) is superimposed over case (2) for conditions at the inclusion surface.

Then, the normal stress is

$$\sigma^r = P_{in}$$

and the tangential stress

$$\sigma^t = 3P/2 - P_{in}/2$$

Radial stress effects can appear if the tangential stress  $\sigma^t$  becomes less than 0 at the inclusion surface, because expansion is taken as negative in the calculation the tangential stress is

$$\sigma^t = 3P/2 - P_{in}/2 \leq 0 \quad (E1)$$

$$P_{in} \geq 3P$$

This is the sufficient condition to cause radial cracks in the matrix around an inclusion.

In the FORTRAN 77 program "Radcra" (D'ARCO and WENDT, 1994) the different  $P$ - $T$  paths were calculated in increments of 0.01 GPa to 0.15 GPa and 5 °C to 50 °C (minimum-maximum increments). These incremental steps allow determination of the final  $P$ - $T$  conditions ( $P_{in} \geq 3P$ ) in the chromite inclusion at which radial cracking can appear as a function of the  $P$ - $T$  starting point and the component of isothermal decompression characteristic for a chosen  $P$ - $T$  path. As shown in figures 5, 6 and 7, all radial cracks appear on lines situated between 0.05 GPa to 0.6 GPa and 40 to 750 °C. Their exact position depends on the  $P$ - $T$  starting conditions. Our calculation is based on three equations following the notation of VAN DER MOLEN and VAN ROERMUND (1986). First we determine the differential volume changes (E2) as a function of the inclusion's thermal expansion ( $\Delta T\alpha_i$ ), the inclusion pressure

$(P_{in}, P_{ii})$  with zero pressure in the host and bulk and shear modulus of the host (C,D).

$$Z = 3 + (\Delta T a_i) \cdot (D - P_{in} C + 3 K_h P_{ii}) \quad (E2)$$

Then, we consider (E3) the thermal expansion of the host ( $\Delta T a_h$ ) as a function of the inclusion's bulk modulus ( $K_i$ ) and the initial inclusion pressure ( $P_{ii}$ ).

$$Y = (3 \Delta T a_h) \cdot (3 K_i - P_{ii}) \quad (E3)$$

To solve the relationship between final pressure and bulk and shear modulus of the host following equation was established (E4).

$$X = D - P^f C \quad (E4)$$

with

$$D = 12 \cdot K_h \cdot \mu_h \text{ and } C = 3 \cdot K_h + 4 \cdot \mu_h$$

These three equations describe the final inclusion pressure as follows:

$$P_i^f = 3 Z K_i - Y X / Z + 3 Y K_h \quad (E5)$$

Equation (E1) shows that tensional normal stress tangential to the inclusion surface arises if the inclusion pressure exceeds three times the pressure applied to the matrix. This condition is fulfilled when

$$\begin{aligned} -\Delta T \Delta \alpha \geq P_h^f (3/2 \mu_h - 1/K_h + 3/K_i) + \\ + P_h (1/K_h - 1/K_i) + \\ + (P_h - P_{ii}) 3/4 \mu_h^{-1} \end{aligned} \quad (E6)$$

#### Parameters for E1 to E6

- $\Delta \alpha$  – Coefficient of volumetric thermal expansion
- $\alpha_i, \alpha_h$  – thermal expansion inclusion, host
- $K_i, K_h$  – bulk modulus inclusion, host
- $P_h$  – initial pressure host
- $P_{ii}$  – initial inclusion pressure
- $P_h^f$  – final pressure in host
- $P_i^f$  – final inclusion pressure
- $\Delta T$  – change in temperature
- $\mu_h$  – shear modulus host

The necessary condition for the general appearance of fractures is discussed by different authors (for example JAEGER and COOK, 1972; NUR and SIMMONS, 1970). Tension can develop around a grain for a limited range of values of the elastic constants. Since the tensile strength is almost zero (at the grain boundary surface), cracks will appear instantaneously.

The tensile strength is

$$\sigma^t = \sqrt{4E\gamma/\pi c},$$

with  $E$  = Young's modulus,

$\gamma$  = fracture surface energy

$c$  = length of the microfractures

This means for grain boundary conditions,

$$\sigma^t = \sqrt{4EV/\pi c} = -P_i/2 \text{ case (1), and } \nu = -P_i^2 \cdot x,$$

with  $x = \pi c/16E$

and

$$\sigma^t = \sqrt{4EV/\pi c} = 3P/2 \text{ case (2), and } \nu = P^2 \cdot y, \text{ with}$$

$y = 9\pi c/16E$

Superposition of case (1) and case (2) for expansion

$$\begin{aligned} \nu &= P_y^2 - P_i^2 x \leq 0, \\ P &\leq P_i \end{aligned}$$

This condition shows that random fractures appear instantaneously, if the inclusion pressure is higher than the external pressure. Figure 4 illustrates the spherical model used for the chromite-olivine inclusion-matrix system and how it works.

The problem posed in this paper was considered using the following parameters:

#### Parameters

(a) Data for chromite	(b) Data for forsterite
$K_0 = 203 \cdot 10^9 \text{ Pa}$	$K_0 = 129 \cdot 10^9 \text{ Pa}$
$\delta K/\delta P = 4.9$	$\delta K/\delta P = 5.1$
	$\mu = 82 \cdot 10^9 \text{ Pa}$

(DUFFY and ANDERSON, 1989)

a = see detailed values:	$\alpha = \text{see detailed values:}$
100 °C, 0.12E-04	96 °C, 0.28E-04
200 °C, 0.13E-04	450 °C, 0.31E-04
400 °C, 0.16E-04	690 °C, 0.33E-04
600 °C, 0.18E-04	963 °C, 0.35E-04
800 °C, 0.21E-04	(SINGH and SIMMONS, 1976)
1000 °C, 0.21E-04	(SKINNER, 1946)

where  $K_0$  = bulk modulus,  $\mu$  = shear modulus,  $\alpha$  = thermal expansion.

Mean diameters  $R_i^2$  for chromite inclusions: 0.12 mm to 0.25 mm (after exhumation).

Mean diameters  $r_2$  for olivine prophyroclasts: 0.7 to 2.0 mm (after exhumation).

P-T starting points for theoretical calculations: 0.7 GPa to 3.0 GPa, 950 °C to 1200 °C.

Qualitative error estimation: the main error introduced in the model is the variation of the petrological data, here the dynamic recrystallization temperature of olivine and the growth of antigorite and tremolite. By using different petrological arguments to constrain the crack filling and the crack overgrowth or the magma crystallization temperature, the error becomes less than 10% of the P-T estimation.